AGU ADVANCING EARTH AND SPACE SCIENCE

Geophysical Research Letters®

RESEARCH LETTER
10.1029/2021GL096767

Key Points:

- Transient simulations of the last deglaciation with the comprehensive Max Planck Institute for Meteorology Earth System Model 1.2
- Glacial climate and millennial-scale climate variability depend significantly on boundary conditions and methods proposed in Paleoclimate Modeling Intercomparison Project - Phase 4 (PMIP4) deglaciation protocol
- Estimating uncertainties for interpretation of differences in PMIP4 model ensemble of the last deglaciation

Supporting Information:

Supporting Information may be found in the online version of this article.

Correspondence to:

M.-L. Kapsch,
marie.kapsch@mpimet.mpg.de

Citation:

Kapsch, M.-L., Mikolajewicz, U., Ziemen, F., & Schannwell, C. (2022). Ocean response in transient simulations of the last deglaciation dominated by underlying ice-sheet reconstruction and method of meltwater distribution. *Geophysical Research Letters*, *49*, e2021GL096767. https://doi.org/10.1029/2021GL096767

Received 29 OCT 2021
Accepted 13 JAN 2022

Ocean Response in Transient Simulations of the Last Deglaciation Dominated by Underlying Ice-Sheet Reconstruction and Method of Meltwater Distribution

Marie-Luise Kapsch[1], Uwe Mikolajewicz[1], Florian Ziemen[1,2], and Clemens Schannwell[1]

[1]Max Planck Institute for Meteorology, Hamburg, Germany, [2]Deutsches Klimarechenzentrum GmbH, Hamburg, Germany

Abstract The last deglaciation was characterized by drastic climate changes, most prominently melting ice sheets. Melting ice sheets have a significant impact on the atmospheric and oceanic circulation, due to changes in the topography and meltwater release into the ocean. In a set of transient simulations of the last deglaciation with the Max Planck Institute for Meteorology Earth System Model we explore differences in the climate response that arise from different boundary conditions and implementations suggested within the Paleoclimate Modeling Intercomparison Project - Phase 4 (PMIP4) deglaciation protocol. The underlying ice-sheet reconstruction dominates the simulated deglacial millennial-scale climate variability in terms of timing and occurrence of observed climate events. Sensitivity experiments indicate that the location and timing of meltwater release from the ice sheets into the ocean are crucial for the ocean response. The results will allow a better interpretation of inter-model differences that arise from different implementations proposed within the PMIP4 protocol.

Plain Language Summary The last deglaciation marked the transition between the last glacial maximum (LGM; about 21,000 years ago) and present. It was characterized by the disappearance of most northern hemispheric ice sheets (e.g., over North America and Eurasia) and a series of abrupt climate events. To investigate the ability of climate models to simulate the last deglaciation and to better understand the physical processes behind the changes, the Paleoclimate Modeling Intercomparison Project - Phase 4 (PMIP4) has designed a common protocol for model simulations of the last deglaciation. This protocol comprises several choices on how to set up the model systems participating in this exercise. With a state-of-the-art climate model, we explore how model simulations of the last deglaciation differ if different boundary data and methods proposed in the protocol are used. Our simulations show that the ice-sheet boundary condition impacts the atmospheric and oceanic circulation during the LGM until about 14,000 years ago. It also determines the timing and occurrence of abrupt climate events throughout the deglaciation. These and further sensitivity experiments presented in this study will help to interpret the differences between model simulations that will be submitted for the PMIP4 deglaciation exercise.

1. Introduction

The last 21 thousand years before present (ka) were characterized by dramatic climate changes, including the retreat of the northern hemispheric ice sheets (Clark et al., 2012). The deglaciation of North America and Eurasia and the retreat of the Antarctic ice sheet resulted in about 130 m global mean sea-level rise (e.g., Lambeck et al., 2014) and significant changes in the atmospheric and oceanic circulation (e.g., Löfverström & Lora, 2017), accompanied by changes in precipitation and temperature patterns (e.g., Kageyama et al., 2021; Löfverström, 2020). Superimposed on these long-term changes were periods of abrupt climate changes, such as a significant northern hemispheric cooling and a slowdown of the Atlantic meridional overturning circulation (AMOC) during Heinrich Event 1 (about 16.8 ka; e.g., Heinrich, 1988; McManus et al., 2004; Stanford et al., 2011) and the Younger Dryas (YD; about 12.8–11.7 ka; e.g., Carlson et al., 2007), or the northern hemispheric warming during the Bølling-Allerød (BA; about 14.7–14.2 ka; e.g., Clark et al., 2002; Weaver et al., 2003).

To understand the mechanisms behind these climate changes the Paleoclimate Modeling Intercomparison Project - Phase 4 (PMIP4; Kageyama et al., 2017) has set up a common protocol for transient simulations of the last deglaciation (Ivanovic et al., 2016). The aim is to study the ability of climate models to retrodict the last deglaciation as recorded from observational evidence and to gain a more comprehensive understanding of the complex and interrelating climate processes that took place during the last deglaciation. To examine uncertainties in deglacial

forcings, trigger mechanisms and dynamic feedbacks the protocol specifies options for different ice-sheet boundary forcing and methods for distributing meltwater from retreating ice sheets. While the latter allows the full range of models to participate in the PMIP4 deglaciation exercise, it is important to disentangle the differences in the model response due to the model setup.

Past studies have investigated the model sensitivity to different ice-sheet boundary conditions (e.g., Bakker et al., 2020; Gong et al., 2015; Hofer et al., 2012; Justino et al., 2005; Liakka & Nilsson, 2010; Liakka et al., 2016; Roe & Lindzen, 2001; Ullman et al., 2014). Using a variety of different model systems, ranging from simplified linear models of the atmosphere to complex fully coupled atmosphere-ocean models, these studies found a strong sensitivity of the modeled climate of the last glacial maximum (LGM; about 21 ka) to the ice-sheet topography. High LGM ice sheets significantly impact the atmospheric and oceanic circulation (see Kageyama & Valdes, 2000; Löfverström & Lora, 2017; Löfverström et al., 2014; Sherriff-Tadano et al., 2018; Zhu et al., 2014). A high Laurentide ice sheet leads to a zonalization and enhancement of the eddy-driven jet stream over the North Atlantic, associated with an increase in surface winds and enhanced wind-driven gyres in the North Atlantic, favoring a stronger AMOC. However, sensitivity experiments by Ullman et al. (2014) and Bakker et al. (2020) showed that the climate response is dependent on the ice-sheet reconstruction used as boundary condition; small deviations in the height of the North American ice sheet between reconstructions can lead to a significantly different atmospheric and oceanic circulation. This indicates that uncertainties in the climate response are largely influenced by the glacial boundary conditions. The inflow of meltwater from retreating ice sheets into the ocean can cause large changes in the AMOC (e.g., McManus et al., 2004), as it potentially reduces the overturning strength. Changes in the AMOC in turn are associated with significant climate changes (Broeker, 1991; Keigwin et al., 1991). Several modeling studies have investigated the response of the AMOC to freshwater forcing in form of so-called hosing experiments (e.g., Kageyama et al., 2010, 2013; Lohmann et al., 2020; Maier-Reimer & Mikolajewicz, 1989; Schiller et al., 1997; Stouffer & Manabe, 2004; Stouffer et al., 2006; Smith & Gregory, 2009). Different methods have been applied to release the freshwater into the ocean, for example, freshwater distribution over latitude belts (Stouffer & Manabe, 2004; Stouffer et al., 2006), certain areas of the North Atlantic or Arctic (Roche et al., 2010; Smith & Gregory, 2009), or point hosing (Condron & Winsor, 2012; Liu et al., 2018; Lohmann et al., 2020; Maier-Reimer & Mikolajewicz, 1989; Schiller et al., 1997). These studies showed that the AMOC is very sensitive to the location of the freshwater hosing. Specifically, it was shown that the AMOC responds more strongly to freshwater if it is released at higher latitudes of the North Atlantic or Arctic, close to or dynamically upstream of the deep water formation sites (Lohmann et al., 2020; Manabe & Stouffer, 1997; Rahmstorf, 1996; Roche et al., 2010; Smith & Gregory, 2009). However, Smith and Gregory (2009) found that if a certain magnitude of freshwater forcing is exceeded the location becomes only of secondary importance and the AMOC responds similarly, independent of where freshwater is added in the North Atlantic.

Using an ensemble of eight transient deglacial simulations with the Max Planck Institute for Meteorology Earth System Model (MPI-ESM), we extend previous studies that investigated the climate response to multiple ice-sheet boundary conditions in time-slice (e.g., Bakker et al., 2020; Liakka et al., 2016; Ullman et al., 2014) and hosing (e.g., Maier-Reimer & Mikolajewicz, 1989; McManus et al., 2004; Stouffer & Manabe, 2004) experiments. We aim to answer how sensitive the transient model climate of the last deglaciation is to the underlying ice-sheet boundary conditions, the implementation of meltwater distribution and the model version. By following the PMIP4 deglaciation protocol, we explore how PMIP4 models might respond to differences in the proposed experimental design. The intention is not to evaluate the simulations in regard to paleo-oceanographic evidence but to highlight differences that arise from the methods proposed in the protocol. This will help to interpret differences in the response of the models participating in the PMIP4 deglaciation exercise. We focus on the Northern Hemisphere, where ice-sheet changes were largest throughout the last deglaciation.

2. Model and Experimental Design

For the transient simulations of the last deglaciation ice sheets were prescribed from two different ice-sheet reconstructions. Meltwater release was calculated from changes in the ice sheet thickness in the reconstructions. To test the sensitivity to the meltwater distribution from melting ice sheets and the sensitivity of the transient climate response to different model parameters, experiments with different methods of meltwater release and model versions were performed, respectively. We apply three model versions, hereafter referred to as P1, P2 and P3. As P2 and P3 include not only a different tuning of parameters than P1 but also different parameterizations and bug

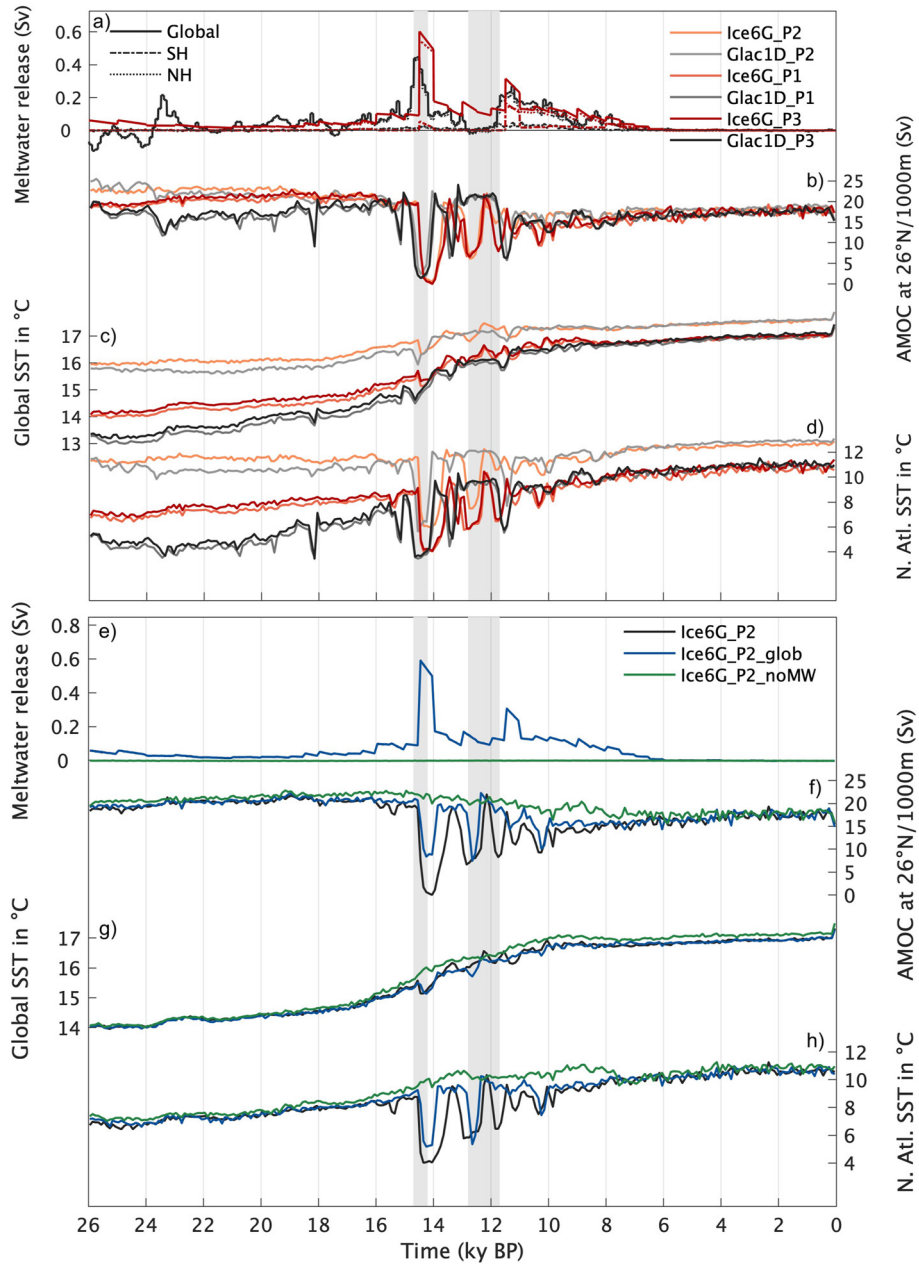

Figure 1. Transient model response to different ice-sheet boundary conditions and implementations of meltwater release for the simulations presented in Table 1. (a) Global (solid) as well as Southern Hemispheric (dashed-dotted) and northern hemispheric (dashed) meltwater release, (b) AMOC at 1,000 m depth and 26°N, (c) global mean sea-surface temperature (SST) and (d) North Atlantic SST for simulations with GLAC-1D (black) and ICE-6G (red) boundary conditions and different model tuning. (e–h) are similar to (a–d) but for simulations with a different meltwater distribution. Vertical shadings mark approximate timings of the Bølling-Allerød (left) and Younger Dryas (right) according to proxy evidence. Note that the global meltwater release time series are identical and overlap for the individual ICE-6G or GLAC-1D experiments.

fixes, we focus our detailed analysis on the simulations with model versions P2 and P3. Details about the model versions are described in Text S1 of Supporting Information S1. The modeled climate differs between versions. P2 and P3 are significantly colder during the glacial than P1, indicating a stronger sensitivity to greenhouse gas changes (Figure 1c). The glacial cooling over the North Atlantic, which is associated with a reduced meridional heat transport due to a weaker AMOC, is more realistic in P2 and P3 than in P1 (Figures 1b and 1d; Tierney et al., 2020). The colder model versions P2 and P3 are also more sensitive to small changes in the meltwater forcing than P1, as they are closer to the temperature threshold at which the AMOC becomes more sensitive to

Table 1
Experiments Performed for This Study

Simulation name	Reconstruction	Meltwater forcing location
Glac1D_P1	GLAC-1D	Local
Glac1D_P2	GLAC-1D	Local
Glac1D_P3	GLAC-1D	Local
Ice6G_P1	ICE-6G	Local
Ice6G_P2	ICE-6G	Local
Ice6G_P3	ICE-6G	Local
Ice6G_P2_Glob	ICE-6G	Global (land and ocean)
Ice6G_P2_noMW	ICE-6G	No meltwater

Note. GLAC-1D and ICE-6G indicate the underlying ice-sheet reconstructions, P1–P3 different parameter tuning within MPI-ESM-CR, and Glob and noMW the meltwater implementation. See Section 2 for details on the experimental design.

perturbations (see discussion in Section 3.1; Klockmann et al., 2018; Oka et al., 2012). All model experiments are summarized in Table 1.

2.1. Model System

The transient simulations were performed with the MPI-ESM version 1.2 in coarse resolution (MPI-ESM-CR; see Mauritsen et al., 2019). The model includes the spectral atmospheric model ECHAM6.3 (Stevens et al., 2013) at T31 horizontal resolution (approx. 3.75°) and 31 vertical levels, the land surface vegetation model JSBACH3.2 (Raddatz et al., 2007), and the primitive equation ocean model MPIOM1.6 (Marsland et al., 2003; Mikolajewicz et al., 2007) with a nominal resolution of 3°. The applied setup was introduced in detail in Kapsch et al. (2021).

2.2. Experimental Design

For each experiment, the model was integrated from a glacial state at 26 ka to the year 1950 with prescribed atmospheric greenhouse gas concentrations (Köhler et al., 2017) and insolation (Berger & Loutre, 1991). Ice sheets and surface topographies were prescribed from either GLAC-1D (Briggs et al., 2014; Tarasov et al., 2012) or ICE-6G (Peltier et al., 2015) reconstructions. All forcing fields are updated every 10 years of the simulations and initiate changes in the topography, glacier mask, river pathways, ocean bathymetry, and land-sea mask (Meccia & Mikolajewicz, 2018; Riddick et al., 2018). For this, all forcing fields are interpolated to a 10-year resolution. For each ice-sheet reconstruction, meltwater from ice sheets is calculated as the temporal derivative of ice thickness at grid points covered by grounded ice sheets (see Figure 1a). The derived meltwater is then distributed by the hydrological discharge model and finally released into the ocean as freshwater (for details, see Meccia & Mikolajewicz, 2018). Thereby salt is conserved and changes in water content within the ESM are consistent with the prescribed ice-sheet changes. In sensitivity experiments, we follow other suggestions within the PMIP4 deglaciation protocol and either distribute meltwater equally over all grid cells (land and ocean) or remove meltwater from the system. For the latter experiment, salt and water are not conserved throughout the simulation.

3. Results and Discussion

Using MPI-ESM-CR, we performed a comprehensive set of sensitivity experiments following the PMIP4 last deglaciation protocol (Ivanovic et al., 2016). We find that the ice-sheet boundary conditions, the method of meltwater distribution and the background climate (realized through different model tuning and parameterizations) play a crucial role for the deglacial climate. While MPI-ESM-CR did not participate in CMIP6/PMIP4 activities, the simulated climate of all experiments presented here fits well within the range of the PMIP4 models for pre-industrial and LGM climate conditions (see Text S2 and Figures S1 and S2 in Supporting Information S1).

3.1. Ice-Sheet Boundary Conditions Crucial for Glacial Climate

Meltwater forcing derived from GLAC-1D and ICE-6G differs significantly in terms of its millennial-scale variability and the timing of major melt events (Figure 1a). These differences partly arise from a different native temporal resolution, which is 100 and 500 years for GLAC-1D and ICE-6G, respectively. For example, the major meltwater pulses (MWP1a and MWP1b at about 14.5 ka and 11.5 ka, respectively) are more confined in GLAC-1D than ICE-6G and the peak discharge occurs at different times. Further, the GLAC-1D meltwater release shows larger variability throughout the last deglaciation. Accordingly, the simulations with GLAC-1D boundary conditions show an enhanced millennial-scale variability over the North Atlantic and globally (Figures 1b–1d). In the following, we focus in more detail on the differences between the simulations with ICE-6G and GLAC-1D reconstructions.

3.1.1. LGM

Although the meltwater history of the two reconstructions before about 15 ka is very similar, except for its millennial-scale variability, the ice-sheet height differs significantly (Figures 1a and 2b; see also Ivanovic et al., 2016). During the LGM, the Laurentide ice sheet is significantly higher in ICE-6G than GLAC-1D and the Fennoscandian/British ice sheet is lower, regionally by more than 950 and 650 m, respectively (Figure 2b). The relatively high Laurentide ice sheet in ICE-6G leads to changes in the zonal 250 hPa wind speed over the North Atlantic, associated with a zonalization and enhancement of the eddy-driven jet stream in the simulations with ICE-6G boundary conditions (Ice6G_P2 and Ice6G_P3; Figure S3 in Supporting Information S1). Similar changes in the 250 hPa winds also occur in Ice6G_P1 but the jet shift is less distinct (Figure S4 in Supporting Information S1). Merz et al. (2015) found that non-topographic forcings, such as orbital forcings, greenhouse gases and sea-surface temperatures can play a crucial role for the jet position. Further, Andres and Tarasov (2019) showed that the jet position is dependent on changes in the background climate through changes in the position of the polar front and sea-ice margin. Our results confirm such sensitivity: Model version P1 shows only a weak cooling over the North Atlantic during the LGM and a less distinct shift of the jet position than P2 and P3 (Figure S4 in Supporting Information S1). The weak cooling of North Atlantic temperatures during the LGM in P1 allows it to maintain a sea-ice margin that is similar to present day (not shown) and thereby a strong and stable AMOC, with a significant North Atlantic deep water cell and deep water formation that is extended toward the eastern North Atlantic (Figure S5 in Supporting Information S1). Hence, the AMOC response to the ice sheet boundary conditions in model version P1 is significantly weaker than in P2 and P3. These findings are in line with Oka et al. (2012) and Klockmann et al. (2018), who showed that a temperature threshold exists at which the AMOC becomes more sensitive to perturbations. The colder model versions P2 and P3 are closer to such temperature threshold and the AMOC is more sensitive to small changes in the forcing than the warmer model. These findings indicate that the model climate affects the atmospheric and oceanic response in the simulations.

The enhancement of the jet in the simulations with ICE-6G ice sheets leads to stronger surface winds and an increase in the wind-driven gyres (Figure S6 in Supporting Information S1). This is associated with an increased northward transport of salty waters and results in a stronger AMOC in the ICE-6G simulations. Hence, a higher Laurentide LGM ice sheet in ICE-6G results in a stronger AMOC (Figure 1), which is in line with Ullman et al. (2014) and other studies (e.g., Kageyama & Valdes, 2000; Löfverström & Lora, 2017; Sherriff-Tadano et al., 2018). The simulations with the GLAC-1D topography do not show a zonalization of the jet stream during the LGM and an enhancement of the wind driven ocean transport. The AMOC in Glac1D_P2 and Glac1D_P3 is more than 4 Sv weaker and North Atlantic surface temperatures are more than 2.6 K lower than in Ice6G_P2 and Ice6G_P3 during the LGM.

Interestingly, we find the largest shifts in the jet over the eastern North Atlantic. Andres and Tarasov (2019) have shown that the jet over the eastern North Atlantic is not very sensitive to the marginal position of the Laurentide ice sheet. This indicates that the shifts of the eastern jet in this study are likely triggered by changes in the stationary waves (e.g., Löfverström et al., 2014), transient eddies (e.g., Merz et al., 2015), and/or wave breaking (Li & Battisti, 2008).

3.1.2. Deglaciation

Due to the reduction in the differences between the ice sheets' height in ICE-6G and GLAC-1D, the differences in temperatures and the AMOC between the simulations with GLAC-1D and ICE-6G boundary conditions get smaller throughout the deglaciation (Figure 1; see also Ullman et al., 2014).

In the reconstructions, an increase in meltwater release mark the onset of the deglaciation (see Figure 1a). However, as the amount of meltwater injected into the ocean is small until the occurrence of MWP1a in both reconstructions, the AMOC remains relatively strong in all simulations until about 14.5 ka (Figure 1b). Interestingly, none of the simulations shows a BA warm period, characterized by a strong AMOC and warm North Atlantic temperatures (Figures 1b and 1d; e.g., Clark et al., 2002; Weaver et al., 2003). Weaver et al. (2003) argued that a MWP1a from Antarctica triggered the BA, as it led to an increase in the strength of North Atlantic deep water formation and thereby an increase in the AMOC. While the source of the meltwater is still debated in the literature (Bentley et al., 2010; Harrison et al., 2019), both reconstructions used in the present study prescribe the largest ice volume changes during MWP1a in the Northern Hemisphere (Figure 1a). A northern hemispheric

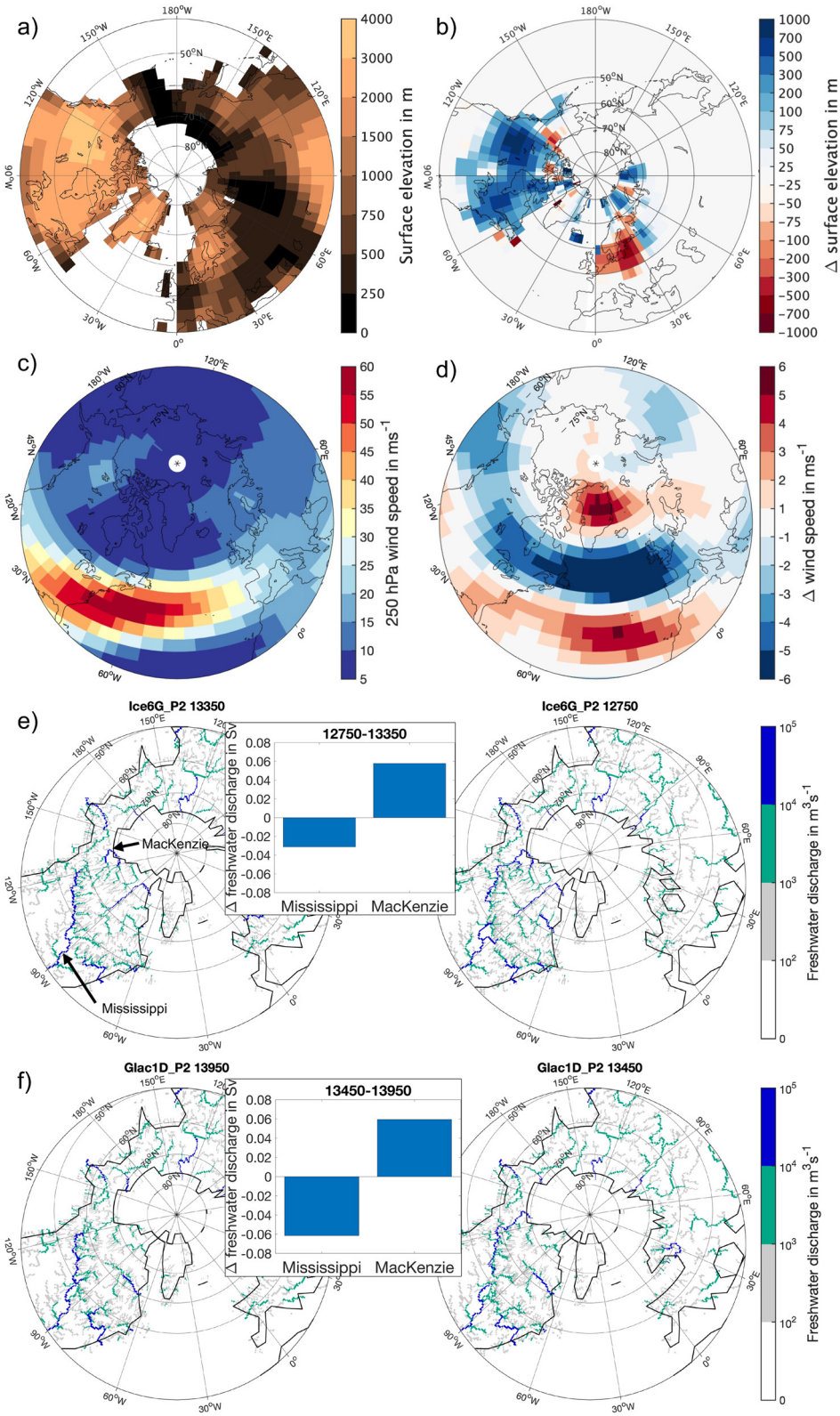
a)
Surface elevation in m
b)
Δ surface elevation in m
c)
250 hPa wind speed in ms^{-1}
d)
Δ wind speed in ms^{-1}
e)
Ice6G_P2 13350
Ice6G_P2 12750
12750-13350
Δ freshwater discharge in Sv
Mississippi
MacKenzie
Freshwater discharge in m^{3}s^{-1}
f)
Glac1D_P2 13950
Glac1D_P2 13450
13450-13950

Figure 2.

meltwater release of more than 0.4 Sv is associated with a significant freshening of the North Atlantic and Arctic ocean (Peltier, 2005), a reduction of the deep water formation and the AMOC in all simulations. Hence, the North Atlantic realms cool significantly and prevents a BA warming in our simulations (Figure 1 and Figure S7 in Supporting Information S1). These findings indicate that the prescribed location of the meltwater pulse in the underlying reconstruction is crucial for the modeled climate response and determines whether a BA warming may occur in deglacial simulations. After the end of MWP1a, the AMOC recovers in the model. In the simulations with GLAC-1D boundary conditions, this AMOC recovery is accompanied with an overshooting of the AMOC, peaking after 200–300 years. While the physical mechanisms of the AMOC slowdowns due to MWP1a in the different simulations are identical, the timing and magnitude of the response is dependent on the underlying reconstruction (Figures 1a–1d; Figure S7 in Supporting Information S1). The peak freshwater discharge of MWP1a occurs about 100 years earlier in GLAC-1D and is about 0.15 Sv weaker than in ICE-6G.

After the AMOC recovery in response to MWP1a and before MWP1b, three additional AMOC slowdowns occur. However, they either occur in simulations with GLAC-1D (about 13.45 ka) or simulations with ICE-6G boundary conditions (about 12.85 ka and 11.75 ka). Note, that the AMOC does not slow down in Glac1D_P1 at 13.45 ka and Ice6G_P1 at 11.75 ka, as model P1 is less sensitive to freshwater changes (see earlier discussion about instability). The AMOC slowdowns are associated with enhanced freshwater discharge into the Arctic due to changes in river directions (Figures 1, 2e, and 2f). Small changes in the topography prescribed from the reconstructions allow a rerouting of meltwater that stems from the Laurentide ice sheet through the MacKenzie instead of the Mississippi river (Figures 2e and 2f). The rerouting leads to a freshening of the Arctic, suppressed overturning and a decrease in AMOC strength. The 11.75 ka event in the simulations with ICE-6G show only small changes in the river directions, but ice-sheet melt occurs mainly at the northeastern side of the Laurentide ice sheet (not shown). This leads to discharge of meltwater into the Labrador Sea and Arctic, hence, a decrease in the AMOC strength. The 12.85 ka event in the simulations with ICE-6G coincides with the YD. Our simulations confirm findings by Condron and Winsor (2012), who suggested that a rerouting of freshwater into the MacKenzie valley led to the AMOC weakening during the YD, as coastal boundary currents effectively transport freshwater from the MacKenzie river toward the deep water formation sites of the subpolar North Atlantic. As no significant increase in meltwater release is evident in ICE-6G during the YD, the results are also in line with previous studies, indicating that no meltwater pulses initiated the YD (Abdul et al., 2016; Stanford et al., 2006; Tarasov & Peltier, 2005).

A meltwater discharge of about 0.3 Sv at 11.45 and 11.25 ka in ICE-6G and GLAC-1D, respectively, characterizes MWP1b (approx. 11.45 ka; Abdul et al., 2016) in the simulations. However, uncertainties of the origin of MWP1b exist (e.g., Bentley et al., 2010; Harrison et al., 2019). In GLAC-1D the largest ice melt during MWP1b occurs in the Northern Hemisphere, while in ICE-6G melt is dominant in the Southern Hemisphere (Figure 1a). In the simulations with GLAC-1D, meltwater discharge into the North Atlantic reduces the North Atlantic deep water formation and leads to a slowdown of the AMOC around the peak of the meltwater discharge (Figure 1). This results in a significant cooling of the Northern Hemisphere, specifically over the North Atlantic (Figures 1a–1d; Figure S7 in Supporting Information S1). In the simulations with ICE-6G, meltwater is released into the Southern Ocean and associated with a cooling of the Southern Hemisphere (Figure 1a and Figure S7 in Supporting Information S1). Interestingly, meltwater release into the Southern Ocean does not significantly affect the AMOC (Figure 1b), which is in line with findings by Stouffer et al. (2007). It also confirms findings by Stanford et al. (2006), who argued that the location of the meltwater injection is more important than the rate and magnitude of the meltwater injection for the North Atlantic deep water formation. The significantly different location of the freshwater release prescribed by the reconstructions explains the fundamental differences in the AMOC response to MWP1b in the simulations with GLAC-1D and ICE-6G reconstructions.

The results emphasize that the climate variability in transient deglacial simulations is largely dependent on the underlying ice-sheet boundary conditions. The height of the reconstructed ice sheets has an influence on the

Figure 2. Differences in the topography between ICE-6G and GLAC-1D lead to changes in the atmospheric circulation and river directions. (a) Surface elevation in ICE-6G and (b) difference in surface elevation between ICE-6G and GLAC-1D and (c) 250 hPa zonal wind speed from Ice6G_P2 and (d) wind-speed difference between Ice6G_P2 and Glac1D_P2 at 21 ka. Note the shift of the projection for the wind speed and underlying present-day coast lines. (e) River routing changes for Ice6G_P2 during the early Younger Dryas: River discharge before the event (left; 13.35 ka) and during the event (right; 12.75 ka); topographic changes lead to an opening and enhanced discharge through the MacKenzie River (inlay). (f) Similar to (e) but for Glac1D_P2 during the 13.45 ka event: River discharge before the event (left; 13.95 ka) and during the event (right; 13.45 ka).

atmospheric circulation during the LGM and early in the deglaciation until about 14 ka, when northern hemispheric ice sheets were still extensive, affecting the wind-driven overturning and the AMOC strength. However, the results also indicate that the meltwater history and changes in river directions dominate the millennial-scale variability in the simulations during the last deglaciation. The reconstructions determine the magnitude, rate and location of meltwater injections, hence, significantly impact the deep water formation in the North Atlantic and the AMOC. These in turn have a significant influence on the northern hemispheric climate (see Figure S7 in Supporting Information S1). Additionally, the model version significantly controls how large the model responds to changes in the boundary conditions.

3.2. Implementation of Meltwater Release Determines Millennial-Scale Variability

The PMIP4 protocol also permits different implementations of meltwater distribution in the experiments (Ivanovic et al., 2016). Sensitivity experiments with a global distribution of meltwater and no meltwater show that the multi-millennial climate variability during the deglaciation is largely controlled by the choice of meltwater implementation (Table 1 and Figures 1e–1h). If meltwater is distributed globally, most AMOC slowdowns throughout the deglaciation still occur (MWP1a, MWP1b, YD). However, a global distribution of meltwater reduces the amount of freshwater that reaches the deep water formation sites in the North Atlantic, resulting in a weaker AMOC response in Ice6G_P2_Glob as compared to Ice6G_P2 (Figure S8 in Supporting Information S1). This indicates that the prescribed meltwater pulses of the aforementioned events are large enough to reduce the overturning strength independent of where freshwater is added in Ice6G_P2_Glob (e.g., Smith & Gregory, 2009; Stanford et al., 2006). It is noteworthy, that the magnitude of the AMOC slowdown during the YD is similar in Ice6G_P2_Glob and Ice6G_P2 but the timing of the AMOC slowdown differs (Figure 1). This indicates that changes in the river directions are likely contributing to an early initiation of the YD AMOC slowdown in Ice6G_P2. However, the persistence of a meltwater peak of more than 0.1 Sv over more than 500 years prescribed from ICE-6G seems large enough to affect the deep water formation in Ice6G_P2_Glob. For other events the AMOC response is fully absent in Ice6G_P2_Glob. For example, the 11.75 ka event is not associated with a long-lived meltwater peak in ICE-6G and the AMOC response in Ice6G_P2 is mainly a result of the discharge into the Labrador Sea and Arctic, hence, the discharge location (see earlier discussion). This emphasizes that a global distribution of relatively small amounts of meltwater does not significantly affect the AMOC in Ice6G_P2_Glob (Figure 1; see also Manabe & Stouffer, 1997; Smith & Gregory, 2009; Rahmstorf, 1996). Additional differences in the AMOC response throughout the deglaciation may arise from the high non-linearity of the AMOC response to changes in greenhouse gases and temperatures (Stouffer & Manabe, 2004; Wang et al., 2002), hence, at times when the CO_2 concentration increases rapidly (see Figure S9 in Supporting Information S1).

In Ice6G_P2_noMW, multi-millennial scale variability is largely absent and the global mean sea-surface temperature is warmer than in Ice6G_P2 from about 16.5 ka onward (Figure 1). As no meltwater pulses are prescribed in Ice6G_P2_noMW that could potentially lead to AMOC slowdowns, an increase in North Atlantic sea-surface temperatures is evident around the BA. The North Atlantic warming is associated with a reorganization of the deep water formation sites throughout the deglaciation as well as a northward shift of the jet stream (see Section 3.1).

4. Conclusions and Implications for PMIP4

Underlying ice-sheet reconstructions and the implementation of meltwater distribution are crucial for the modeled climate response in transient simulations of the last deglaciation. These results are obtained by performing an ensemble of eight transient simulations with the state-of-the-art MPI-ESM in coarse resolution. MPI-ESM-CR is most suitable for transient simulations, as it accounts for changes in the topography, glacier mask, river pathways, ocean bathymetry, and land-sea mask. The objective of this study is to compare the climatic impact from the different methods proposed in the PMIP4 deglaciation protocol (Ivanovic et al., 2016) and to highlight the uncertainties that arise from different boundary conditions. A more thorough analysis of the associated physical processes is essential and will be conducted in a future study.

Specifically, we find that differences in the topography between ICE-6G and GLAC-1D significantly impact the atmospheric circulation. With glacial ICE-6G ice sheets the Atlantic jet in the Northern Hemisphere shows higher wind speeds and a more zonal and equatorward position (e.g., Merz et al., 2015). Glacial GLAC-1D ice

sheets are lower and do not lead to changes in the jet position. Hence, the ocean response significantly differs between the simulations with ICE-6G and GLAC-1D. Small changes in the topography throughout the deglaciation affect changes in river directions and explain substantial differences in the climate response between simulations. For example, during the YD a rerouting of meltwater from the Mississippi into the Arctic is evident in the simulations, but only ICE-6G reconstructions prescribe a sufficient amount of melt water to significantly affect the ocean circulation. Therefore, a YD cooling is only evident in simulations with ICE-6G. Other observed climate events, such as the BA warm period, are not simulated in the experiments with prescribed meltwater, as MWP1a is released in the Northern Hemisphere in both reconstructions, where it leads to a reduction in the AMOC strength and a significant cooling. Sensitivity experiments with different model versions show that the background climate is essential for the ocean response in the simulations, as it determines how close the AMOC is to the bifurcation point between a strong and weak AMOC (Klockmann et al., 2018; Oka et al., 2012). These findings are in line with previous studies, investigating the effect of ice-sheet boundary conditions on the atmospheric and oceanic circulation (e.g., Bakker et al., 2020; Löfverström et al., 2014; Merz et al., 2015; Pausata et al., 2011; Ullman et al., 2014) and the importance of meltwater injections for the AMOC stability (e.g., Stanford et al., 2006; Stouffer et al., 2007). Performing a first systematic ensemble of transient simulations with different ice-sheet boundary conditions and methods of meltwater distribution, the present study extends previous studies and shows that differences in the topography and meltwater history of ICE-6G and GLAC-1D dominate the simulated millennial-scale climate variability in simulations of the last deglaciation.

The PMIP4 deglaciation protocol is designed for a large range of models to participate in the exercise. Most modeling groups will likely only contribute to PMIP4 with a subset of the simulations presented here, due to computational or technical limitations. Our experiments point toward the challenges in interpreting results from simulations with the different methods proposed in the PMIP4 deglaciation protocol, as the differences in the climate response due to the implementation choices proposed in the protocol can be as large as the climate variability that the simulations try to capture. Further, a direct comparison of the model results with proxy evidence will be difficult, as the proposed boundary conditions do not allow for the modeling of all observed climate events (e.g., BA), and the climate effect arising from the uncertainties in the ice-sheet reconstructions is large. This points toward the necessity of a more process-based analysis and interpretation of the PMIP4 last deglaciation ensemble.

Data Availability Statement

Model data and scripts used for the analysis will be available online on the MPG.PuRe repository (http://hdl.handle.net/21.11116/0000-0009-128D-4) upon publication. Post-processed Paleoclimate Modeling Intercomparison Project - Phase four model data by LSCE is available at http://dods.lsce.ipsl.fr/pmip4/db/ (last access: 13 December 2021). Max Planck Institute Earth System Model model code is available upon request from the Max Planck Institute for Meteorology (reinhard.budich@mpimet.mpg.de) under the Software License Agreement version 2 (https://mpimet.mpg.de/en/science/modeling-with-icon/code-availability - last access: 25 August 2021). Additionally, the full model output will be made available on the ESGF repository.

Acknowledgments
The project was funded by the German Federal Ministry of Education and Research as a Research for Sustainability Initiative through the PalMod project (grant nos. 01LP1504C, 01LP1502A, 01LP1915C, and 01LP1917B). All Max Planck Institute for Meteorology Earth System Model simulations were performed at the German Climate Computing Center. The authors would also like to thank the Laboratoire des Sciences du Climate et de l'environment for providing post-processed Paleoclimate Modeling Intercomparison Project - Phase 4 data and acknowledge two anonymous reviewers as well as the editor Gudrun Magnusdottir, who have helped to improve our manuscript. Open access funding enabled and organized by Projekt DEAL.

References

Abdul, N. A., Mortlock, R. A., Wright, J. D., & Fairbanks, R. G. (2016). Younger Dryas sea level and meltwater pulse 1b recorded in Barbados reef crest coral *Acropora palmata*. *Paleoceanography*, *31*(2), 330–344. https://doi.org/10.1002/2015pa002847

Andres, H. J., & Tarasov, L. (2019). Towards understanding potential atmospheric contributions to abrupt climate changes: Characterizing changes to the North Atlantic eddy-driven jet over the last deglaciation. *Climate of the Past*, *15*(4), 1621–1646. https://doi.org/10.5194/cp-15-1621-2019

Bakker, P., Rogozhina, I., Merkel, U., & Prange, M. (2020). Hypersensitivity of glacial summer temperatures in Siberia. *Climate of the Past*, *16*(1), 371–386. https://doi.org/10.5194/cp-16-371-2020

Bentley, M. J., Fogwill, C. J., Brocq, A. M. L., Hubbard, A. L., Sugden, D. E., Dunai, T. J., & Freeman, S. P. (2010). Deglacial history of the west Antarctic ice sheet in the Weddell Sea embayment: Constraints on past ice volume change. *Geology*, *38*(5), 411–414. https://doi.org/10.1130/G30754.1

Berger, A., & Loutre, M. (1991). Insolation values for the climate of the last 10 million years. *Quaternary Science Reviews*, *10*(4), 297–317. https://doi.org/10.1016/0277-3791(91)90033-q

Briggs, R. D., Pollard, D., & Tarasov, L. (2014). A data-constrained large ensemble analysis of Antarctic evolution since the Eemian. *Quaternary Science Reviews*, *103*, 91–115. https://doi.org/10.1016/j.quascirev.2014.09.003

Broeker, W. (1991). The great ocean conveyor. *Oceanography*, *4*(2), 79–89. https://doi.org/10.5670/oceanog.1991.07

Carlson, A. E., Clark, P. U., Haley, B. A., Klinkhammer, G. P., Simmons, K., Brook, E. J., & Meissner, K. J. (2007). Geochemical proxies of North American freshwater routing during the Younger Dryas cold event. *Proceedings of the National Academy of Sciences*, *104*(16), 6556–6561. https://doi.org/10.1073/pnas.0611313104

Clark, P. U., Pisias, N. G., Stocker, T. F., & Weaver, A. J. (2002). The role of the thermohaline circulation in abrupt climate change. *Nature*, *415*(6874), 863–869. https://doi.org/10.1038/415863a

Clark, P. U., Shakun, J. D., Baker, P. A., Bartlein, P. J., Brewer, S., Brook, E., et al. (2012). Global climate evolution during the last deglaciation. *Proceedings of the National Academy of Sciences*, *109*(19), E1134–E1142. https://doi.org/10.1073/pnas.1116619109

Condron, A., & Winsor, P. (2012). Meltwater routing and the Younger Dryas. *Proceedings of the National Academy of Sciences*, *109*(49), 19928–19933. https://doi.org/10.1073/pnas.1207381109

Gong, X., Zhang, X., Lohmann, G., Wei, W., Zhang, X., & Pfeiffer, M. (2015). Higher Laurentide and Greenland ice sheets strengthen the North Atlantic Ocean circulation. *Climate Dynamics*, *45*(1–2), 139–150. https://doi.org/10.1007/s00382-015-2502-8

Harrison, S., Smith, D. E., & Glasser, N. F. (2019). Late quaternary meltwater pulses and sea level change. *Journal of Quaternary Science*, *34*(1), 1–15. https://doi.org/10.1002/jqs.3070

Heinrich, H. (1988). Origin and consequences of cyclic ice rafting in the Northeast Atlantic Ocean during the past 130,000 years. *Quaternary Research*, *29*(2), 142–152. https://doi.org/10.1016/0033-5894(88)90057-9

Hofer, D., Raible, C. C., Dehnert, A., & Kuhlemann, J. (2012). The impact of different glacial boundary conditions on atmospheric dynamics and precipitation in the North Atlantic region. *Climate of the Past*, *8*(3), 935–949. https://doi.org/10.5194/cp-8-935-2012

Ivanovic, R. F., Gregoire, L. J., Kageyama, M., Roche, D. M., Valdes, P. J., Burke, A., et al. (2016). Transient climate simulations of the deglaciation 21–9 thousand years before present (version 1) – PMIP4 core experiment design and boundary conditions. *Geoscientific Model Development*, *9*(7), 2563–2587. https://doi.org/10.5194/gmd-9-2563-2016

Justino, F., Timmermann, A., Merkel, U., & Souza, E. P. (2005). Synoptic reorganization of atmospheric flow during the last glacial maximum. *Journal of Climate*, *18*(15), 2826–2846. https://doi.org/10.1175/jcli3403

Kageyama, M., Albani, S., Braconnot, P., Harrison, S. P., Hopcroft, P. O., Ivanovic, R. F., et al. (2017). The PMIP4 contribution to CMIP6 – Part 4: Scientific objectives and experimental design of the PMIP4-CMIP6 last glacial maximum experiments and PMIP4 sensitivity experiments. *Geoscientific Model Development*, *10*(11), 4035–4055. https://doi.org/10.5194/gmd-10-4035-2017

Kageyama, M., Harrison, S. P., Kapsch, M. L. L., Löfverström, M., Lora, J. M., Mikolajewicz, U., & Volodin, E. (2021). The PMIP4-CMIP6 last glacial maximum experiments: Preliminary results and comparison with the PMIP3-CMIP5 simulations. *Climate of the Past*, *17*(3), 1065–1089. https://doi.org/10.5194/cp-2019-169

Kageyama, M., Merkel, U., Otto-Bliesner, B., Prange, M., Abe-Ouchi, A., Lohmann, G., et al. (2013). Climatic impacts of fresh water hosing under last glacial maximum conditions: A multi-model study. *Climate of the Past*, *9*(2), 935–953. https://doi.org/10.5194/cp-9-935-2013

Kageyama, M., Paul, A., Roche, D. M., & Van Meerbeeck, C. J. (2010). Modelling glacial climatic millennial-scale variability related to changes in the Atlantic meridional overturning circulation: A review. *Quaternary Science Reviews*, *29*(21), 2931–2956. https://doi.org/10.1016/j.quascirev.2010.05.029

Kageyama, M., & Valdes, P. J. (2000). Impact of the North American ice-sheet orography on the last glacial maximum eddies and snowfall. *Geophysical Research Letters*, *27*(10), 1515–1518. https://doi.org/10.1029/1999gl011274

Kapsch, M. L., Mikolajewicz, U., Ziemen, F. A., Rodehacke, C. B., & Schannwell, C. (2021). Analysis of the surface mass balance for deglacial climate simulations. *The Cryosphere*, *15*(2), 1131–1156. https://doi.org/10.5194/tc-15-1131-2021

Keigwin, L. D., Jones, G. A., Lehman, S. J., & Boyle, E. A. (1991). Deglacial meltwater discharge, North Atlantic Deep Circulation, and abrupt climate change. *Journal of Geophysical Research*, *96*(C9), 16811–16826. https://doi.org/10.1029/91jc01624

Klockmann, M., Mikolajewicz, U., & Marotzke, J. (2018). Two AMOC states in response to decreasing greenhouse gas concentrations in the coupled climate model MPI-ESM. *Journal of Climate*, *31*(19), 7969–7984. https://doi.org/10.1175/JCLI-D-17-0859.1

Köhler, P., Nehrbass-Ahles, C., Schmitt, J., Stocker, T. F., & Fischer, H. (2017). A 156 kyr smoothed history of the atmospheric greenhouse gases CO_2, CH_4, and N_2O and their radiative forcing. *Earth System Science Data*, *9*(1), 363–387. https://doi.org/10.5194/essd-9-363-2017

Lambeck, K., Rouby, H., Purcell, A., Sun, Y., & Sambridge, M. (2014). Sea level and global ice volumes from the last glacial maximum to the Holocene. *Proceedings of the National Academy of Sciences*, *111*(43), 15296–15303. https://doi.org/10.1073/pnas.1411762111

Li, C., & Battisti, D. S. (2008). Reduced Atlantic storminess during last glacial maximum: Evidence from a coupled climate model. *Journal of Climate*, *21*(14), 3561–3579. https://doi.org/10.1175/2007jcli2166.1

Liakka, J., Löfverström, M., & Colleoni, F. (2016). The impact of the North American glacial topography on the evolution of the Eurasian ice sheet over the last glacial cycle. *Climate of the Past*, *12*(5), 1225–1241. https://doi.org/10.5194/cp-12-1225-2016

Liakka, J., & Nilsson, J. (2010). The impact of topographically forced stationary waves on local ice-sheet climate. *Journal of Glaciology*, *56*(197), 534–544. https://doi.org/10.3189/002214310792447824

Liu, Y., Hallberg, R., Sergienko, O., Samuels, B. L., Harrison, M., & Oppenheimer, M. (2018). Climate response to the meltwater runoff from Greenland ice sheet: Evolving sensitivity to discharging locations. *Climate Dynamics*, *51*(5), 1733–1751. https://doi.org/10.1007/s00382-017-3980-7

Löfverström, M. (2020). A dynamic link between high-intensity precipitation events in southwestern North America and Europe at the Last Glacial Maximum. *Earth and Planetary Science Letters*, *534*, 116081. https://doi.org/10.1016/j.epsl.2020.116081

Löfverström, M., Caballero, R., Nilsson, J., & Kleman, J. (2014). Evolution of the large-scale atmospheric circulation in response to changing ice sheets over the last glacial cycle. *Climate of the Past*, *10*(4), 1453–1471. https://doi.org/10.5194/cp-10-1453-2014

Löfverström, M., & Lora, J. M. (2017). Abrupt regime shifts in the North Atlantic atmospheric circulation over the last deglaciation. *Geophysical Research Letters*, *44*(15), 8047–8055. https://doi.org/10.1002/2017gl074274

Lohmann, G., Butzin, M., Eissner, N., Shi, X., & Stepanek, C. (2020). Abrupt climate and weather changes across time scales. *Paleoceanography and Paleoclimatology*, *35*(9), e2019PA003782. https://doi.org/10.1029/2019pa003782

Maier-Reimer, E., & Mikolajewicz, U. (1989). *Experiments with an OGCM on the cause of the Younger Dryas* (Vol. 39).

Manabe, S., & Stouffer, R. J. (1997). Coupled ocean-atmosphere model response to freshwater input: Comparison to Younger Dryas Event. *Paleoceanography*, *12*(2), 321–336. https://doi.org/10.1029/96pa03932

Marsland, S., Haak, H., Jungclaus, J., Latif, M., & Röske, F. (2003). The Max-Planck-Institute global ocean/sea ice model with orthogonal curvilinear coordinates. *Ocean Modelling*, *5*(2), 91–127. https://doi.org/10.1016/s1463-5003(02)00015-x

Mauritsen, T., Bader, J., Becker, T., Behrens, J., Bittner, M., Brokopf, R., et al. (2019). Developments in the MPI-M earth system model version 1.2 (MPI-ESM1.2) and its response to increasing CO_2. *Journal of Advances in Modeling Earth Systems*, *11*(4), 998–1038. https://doi.org/10.1029/2018ms001400

Mauritsen, T., & Roeckner, E. (2020). Tuning the MPI-ESM1.2 global climate model to improve the match with instrumental record warming by lowering its climate sensitivity. *Journal of Advances in Modeling Earth Systems*, *12*(5), e2019MS002037. https://doi.org/10.1029/2019ms002037

McManus, J. F., Francois, R., Gherardi, J. M., Keigwin, L. D., & Brown-Leger, S. (2004). Collapse and rapid resumption of Atlantic meridional circulation linked to deglacial climate changes. *Nature*, *428*(6985), 834–837. https://doi.org/10.1038/nature02494

Meccia, V. L., & Mikolajewicz, U. (2018). Interactive ocean bathymetry and coastlines for simulating the last deglaciation with the Max Planck Institute earth system model (MPI-ESM-v1.2). *Geoscientific Model Development*, *11*(11), 4677–4692. https://doi.org/10.5194/gmd-11-4677-2018

Merz, N., Raible, C. C., & Woollings, T. (2015). North Atlantic eddy-driven jet in interglacial and glacial winter climates. *Journal of Climate*, *28*(10), 3977–3997. https://doi.org/10.1175/jcli-d-14-00525.1

Mikolajewicz, U., Gröger, M., Maier-Reimer, E., Schurgers, G., Vizcaíno, M., & Winguth, A. M. E. (2007). Long-term effects of anthropogenic CO_2 emissions simulated with a complex earth system model. *Climate Dynamics*, *28*(6), 599–633. https://doi.org/10.1007/s00382-006-0204-y

Oka, A., Hasumi, H., & Abe-Ouchi, A. (2012). The thermal threshold of the Atlantic meridional overturning circulation and its control by wind stress forcing during glacial climate. *Geophysical Research Letters*, *39*(9). https://doi.org/10.1029/2012gl051421

Pausata, F. S. R., Li, C., Wettstein, J. J., Kageyama, M., & Nisancioglu, K. H. (2011). The key role of topography in altering North Atlantic atmospheric circulation during the last glacial period. *Climate of the Past*, *7*(4), 1089–1101. https://doi.org/10.5194/cp-7-1089-2011

Peltier, W. R. (2005). On the hemispheric origins of meltwater pulse 1a. *Quaternary Science Reviews*, *24*(14), 1655–1671. https://doi.org/10.1016/j.quascirev.2004.06.023

Peltier, W. R., Argus, D. F., & Drummond, R. (2015). Space geodesy constrains ice age terminal deglaciation: The global ICE-6G_C (VM5a) model. *Journal of Geophysical Research: Solid Earth*, *120*(1), 450–487. https://doi.org/10.1002/2014jb011176

Raddatz, T. J., Reick, C. H., Knorr, W., Kattge, J., Roeckner, E., Schnur, R., et al. (2007). Will the tropical land biosphere dominate the climate–carbon cycle feedback during the twenty-first century? *Climate Dynamics*, *29*(6), 565–574. https://doi.org/10.1007/s00382-007-0247-8

Rahmstorf, S. (1996). On the freshwater forcing and transport of the Atlantic thermohaline circulation. *Climate Dynamics*, *12*(12), 799–811. https://doi.org/10.1007/s003820050144

Riddick, T., Brovkin, V., Hagemann, S., & Mikolajewicz, U. (2018). Dynamic hydrological discharge modelling for coupled climate model simulations of the last glacial cycle: The MPI-DynamicHD model version 3.0. *Geoscientific Model Development*, *11*(10), 4291–4316. https://doi.org/10.5194/gmd-11-4291-2018

Roche, D. M., Wiersma, A. P., & Renssen, H. (2010). A systematic study of the impact of freshwater pulses with respect to different geographical locations. *Climate Dynamics*, *34*(7). https://doi.org/10.1007/s00382-009-0578-8

Roe, G. H., & Lindzen, R. S. (2001). The mutual interaction between continental-scale ice sheets and atmospheric stationary waves. *Journal of Climate*, *14*(7), 1450–1465. https://doi.org/10.1175/1520-0442(2001)014<1450:tmibcs>2.0.co;2

Schiller, A., Mikolajewicz, U., & Voss, R. (1997). The stability of the North Atlantic thermohaline circulation in a coupled ocean-atmosphere general circulation model. *Climate Dynamics*, *13*(13), 325–347. https://doi.org/10.1007/s003820050169

Sherriff-Tadano, S., Abe-Ouchi, A., Yoshimori, M., Oka, A., & Chan, W. L. (2018). Influence of glacial ice sheets on the Atlantic meridional overturning circulation through surface wind change. *Climate Dynamics*, *50*, 2881–2903. https://doi.org/10.1007/s00382-017-3780-0

Smith, R. S., & Gregory, J. M. (2009). A study of the sensitivity of ocean overturning circulation and climate to freshwater input in different regions of the North Atlantic. *Geophysical Research Letters*, *36*(15). https://doi.org/10.1029/2009gl038607

Stanford, J. D., Rohling, E. J., Bacon, S., Roberts, A. P., Grousset, F. E., & Bolshaw, M. (2011). A new concept for the paleoceanographic evolution of Heinrich event 1 in the North Atlantic. *Quaternary Science Reviews*, *30*(9), 1047–1066. https://doi.org/10.1016/j.quascirev.2011.02.003

Stanford, J. D., Rohling, E. J., Hunter, S. E., Roberts, A. P., Rasmussen, S. O., Bard, E., & Fairbanks, R. G. (2006). Timing of meltwater pulse 1a and climate responses to meltwater injections. *Paleoceanography*, *21*(4). https://doi.org/10.1029/2006pa001340

Stevens, B., Giorgetta, M., Esch, M., Mauritsen, T., Crueger, T., Rast, S., et al. (2013). Atmospheric component of the MPI-M earth system model: ECHAM6. *Journal of Advances in Modeling Earth Systems*, *5*(2), 146–172. https://doi.org/10.1002/jame.20015

Stouffer, R. J., & Manabe, S. (2004). Equilibrium response of thermohaline circulation to large changes in atmospheric CO_2 concentration. *Climate Dynamics*, *22*(2), 325–326. https://doi.org/10.1007/s00382-004-0394-0

Stouffer, R. J., Seidov, D., & Haupt, B. J. (2007). Climate response to external sources of freshwater: North Atlantic versus the Southern Ocean. *Journal of Climate*, *20*(3), 436–448. https://doi.org/10.1175/jcli4015.1

Stouffer, R. J., Yin, J., Gregory, J. M., Dixon, K. W., Spelman, M. J., Hurlin, W., et al. (2006). Investigating the causes of the response of the thermohaline circulation to past and future climate changes. *Journal of Climate*, *19*(8), 1365–1387. https://doi.org/10.1175/jcli3689.1

Tarasov, L., Dyke, A. S., Neal, R. M., & Peltier, W. (2012). A data-calibrated distribution of deglacial chronologies for the North American ice complex from glaciological modeling. *Earth and Planetary Science Letters*, *315–316*, 30–40. https://doi.org/10.1016/j.epsl.2011.09.010

Tarasov, L., & Peltier, W. R. (2005). Arctic freshwater forcing of the Younger Dryas cold reversal. *Nature*, *435*(7042), 662–665. https://doi.org/10.1038/nature03617

Tierney, J. E., Zhu, J., King, J., Malevich, S. B., Hakim, G. J., & Poulsen, C. J. (2020). Glacial cooling and climate sensitivity revisited. *Nature*, *584*, 569–573. https://doi.org/10.1038/s41586-020-2617-x

Ullman, D. J., LeGrande, A. N., Carlson, A. E., Anslow, F. S., & Licciardi, J. M. (2014). Assessing the impact of Laurentide Ice Sheet topography on glacial climate. *Climate of the Past*, *10*(2), 487–507. https://doi.org/10.5194/cp-10-487-2014

Wang, Z., Mysak, L. A., & McManus, J. F. (2002). Response of the thermohaline circulation to cold climates. *Paleoceanography*, *17*(1), 6-1–6-14. https://doi.org/10.1029/2000pa000587

Weaver, A. J., Saenko, O. A., Clark, P. U., & Mitrovica, J. X. (2003). Meltwater pulse 1a from Antarctica as a trigger of the Bølling-Allerød warm interval. *Science*, *299*(5613), 1709–1713. https://doi.org/10.1126/science.1081002

Zhu, J., Liu, Z., Zhang, X., Eisenman, I., & Liu, W. (2014). Linear weakening of the AMOC in response to receding glacial ice sheets in CCSM3. *Geophysical Research Letters*, *41*(17), 6252–6258. https://doi.org/10.1002/2014gl060891